RSC Advances

ROYAL SOCIETY OF CHEMISTRY

www.rsc.org/advances

RSC Advances

ARTICLE

Potential applications of abandoned aromatic polyamide reverse osmosis membrane by hypochlorite degradation

Received 00th January 20xx,
Accepted 00th January 20xx

DOI: 10.1039/x0xx00000x

www.rsc.org/

Ganning Zeng[a], Guannan Lian[a], Yicheng Zhang[a], Lu Gan[a], Yong Zhou[a,b], Junhong Qiu[a], Bart van der Bruggen[c,d], Jiangnan Shen*[a, b]

Reverse osmosis (RO) membranes might experience significant changes in surface structure and performance after disinfection has been applied, or after membrane cleaning, because of hydrolysis and oxidation processes. This study reports potential applications of aromatic polyamide RO membrane exposed to a sodium hypochlorite solution for desalination of dye solutions. Changes in the chemical composition, morphology and performance of such membrane were characterized by Fourier transform infrared spectroscopy (FT-IR), X-ray photoelectron spectroscopy (XPS), contact angle measurements, scanning electron microscope (SEM), atomic force microscopy (AFM) and streaming potential measurements. After chlorination, the water flux of RO membrane doubled, and the NaCl and Na_2SO_4 rejection of the RO membrane decreased to 46.2 % and 86.2 %, respectively. However, the rejection of congo red, methyl blue and direct red 80 were 99.4 %, 98.0 % and 100 %, respectively. This indicates that abandoned RO membranes can be recovered as "nanofiltration functional membranes" after sodium hypochlorite exposure, and be suitable for fractionation purposes.

1. Introduction

Reverse osmosis (RO) membranes are extensively applied in desalination in order to satisfy the growing requirement for fresh water worldwide.[1] However, RO membranes are easily polluted and oxidized, which limits their normal operation.[2] Disinfection and chemical cleaning are usually applied to prevent biofouling and to rejuvenate membranes. This is typically done by chlorine or hypochlorite pretreatment. However, most aromatic polyamide RO membranes are very sensitive to residual chlorine. Gradual membrane degradation may occur in an oxidizing environment due to the presence of free chlorine, particularly over a long period of time.[3-6] The polyamide active layers of RO membranes can be modified by active chlorine species; chlorine concentration and a high or low pH may also alter the membrane hydrophilicity, either increase or decrease.[7-10] Van Thanh Do et al.[11] concluded that the changes in membrane performance resulted from chlorination could be explained as competing mechanism, which included membrane tightening, charge repulsion, and chlorination induced polyamide hydrolysis. These effects may potentially explain reported contradictory observations. However, the effects of biocides on the performance and the operational life span of membranes are mainly elucidated based on size exclusion and charge repulsion. Further implications on the oxidation and degradation mechanisms of polyamide membrane by morphological and chemical analysis are still poorly understood. In industrial practice, RO membranes are abandoned when a performance reduction in observed, especially for water permeability and salt rejection. This causes not only a vast resource waste, but also a large of operational cost of desalination. However, these abandoned aromatic polyamide RO membranes can be recovered as "Nanofiltration functional membranes" by hydrolyzation and oxidation and applied in the separation of salts and organic solutes. Jing et al.[12] proposed that oxidative modified RO membranes have a similar performance of removing monovalent ions, divalent ions and macromolecule organic as nanofiltration (NF) membranes, operating at low operational pressure.

Membrane technologies for fractionation of dye solutions have been proven to be effective, especially aiming at cleaner production and resource recovery.[13-15] The past few decades have witnessed remarkable applications of membranes on treatment of dye effluents[16], in which nanofiltration membranes are particularly advantageous, mainly because of their superior properties such as fine pore size, charge repulsion, large specific surface area, high porosity, stability in liquid media, and capability of overcoming the huge power cost when high pressure RO membrane is applied. However, the large cost of production is still a hurdle for the application of nanofiltration membranes. Therefore, "Nanofiltration functional membranes" obtained by degradation of abandoned polyamide RO membranes may be a plausible approach to reduce the cost of membrane manufacturing.

[a] Ocean College, Zhejiang University of Technology, Hangzhou 310014, China
[b] Center for membrane separation and water science & technology, Zhejiang University of Technology, Hangzhou 310014, China
[c] Department of Chemical Engineering, KU Leuven, Celestijinenlaan 200F, B-3001 Leuven, Belgium
[d] Faculty of Engineering and the Built Environment, Tshwane University of Technology, Private Bag X680, Pretoria 0001, South Africa
† Electronic Supplementary Information (ESI) available. See DOI: 10.1039/x0xx00000x

The aim of this study was to obtain "Nanofiltration functional membranes" via sodium hypochlorite degradation of abandoned polyamide RO membranes. Changes of membrane surface properties under chlorine exposure were analyzed by FT-IR, XPS, SEM, AFM, contact angle measurements and streaming potential measurements. The performance of "Nanofiltration functional membranes" for desalination of dye solutions was studied. Furthermore, the influence of the operational pressure, dye concentrations and feeding salt concentration on the separation capability of "Nanofiltration functional membranes" was investigated.

2. Experimental

2.1 Membranes and reagents

2.1.1 Polyamide RO membranes

The aromatic polyamide RO membranes used in this investigation were obtained from the Hangzhou Water Treatment Technology Development Center, which were fabricated by the method of interfacial polymerization on polysulfone layers. The main properties of original membranes are as follows: permeate flux 59.6 ± 1.6 L m^{-2} h^{-1} and the NaCl rejection 97.6 ± 0.3 %. All membranes were stored at 0.5 % $NaHSO_3$ solution before using.

2.1.2 Reagents

Sodium hypochlorite (effective chlorine content: ~ 10 %) was used for exposure of membrane to chlorine. Different dyes, including congo red (> 98.0 %, Aladdin), methyl blue (AR, Aladdin), direct red 80 (AR, Aladdin) and raffinose (99.0 %, Aladdin) were used in the experiments. Detailed information of these dyes is shown in Table 1. Deionized water was used in all experiments.

2.2 Membrane degradation protocol

Sodium hypochlorite solutions were prepared in a concentration of 1000 ppm and at a pH of 11.5. Because the pK_a of hypochlorous acid is ~ 7.5, the main active species is ClO^- at this pH.[8] Membranes used in the experiments were immersed in beakers containing a sodium hypochlorite solution of 1000 ppm for 48 h at constant temperature (27 °C), and beakers were placed in darkness to avoid photochemical degradation of sodium hypochlorite solution. Their performance was tested after being thoroughly rinsed and soaked in deionized water for 12 h.

2.3 Membrane surface analysis

2.3.1 Morphological analysis

SEM (SIRION-100, FEI, Netherlands) and AFM (VEECO, America) were used to characterize the membrane surface morphology. The roughness of the original and chlorinated polyamide active layers was estimated from the topography image of an area using AFM. Surface topography was detected using a contact mode in air medium. The average roughness value was calculated by three random area scans.

2.3.2 Chemical analysis

XPS and FT-IR were applied to explore the changes in surface composition of the chlorinated membranes. XPS was accomplished on Kratos Axis-Ultra DLD spectrometer, using a monochromatic Al Kα source (hu = 1487 eV). XPS full-scan spectra were recorded within the range from 0 to 1400 eV with 1 eV resolution. FT-IR analysis was conducted by a Nicolet 6700 spectrometer. The original and chlorinated membranes were scanned within the range from 400 to 4000 cm^{-1}.

2.3.3 Contact angle and streaming potential measurements

The contact angle was measured with a Dataphysics Instruments OCA 30 Goniometer (Filderstadt, Germany). A sessile drop technique was accomplished by 10 μL Milli-Q water on the surface of the membrane at room temperature. The reported contact angles of the membranes were calculated by the average results of 5 measurements on the randomly selected membrane surface.

Streaming potentials were obtained by a SurPASS electrokinetic analyzer (Anton Parr, Austria). All streaming potentials were measured with a 10 mM KCl solution. The zeta potential was calculated in Fairbrother-Mastin approach.

2.4 Evaluation of membrane performance

Experiments were performed at 1 MPa with solution containing 500 mg/L NaCl, 500 mg/L Na_2SO_4, 200 mg/L congo red dye, 200 mg/L methyl blue dye, 200 mg/L direct red 80 dye and 1 g/L raffinose, respectively. Original membranes and chlorinated membranes were soaked and rinsed thoroughly with deionized water and were pressurized at 1.0 MPa for one hour to get a steady flux. A laboratory-scale cross-flow filtration apparatus were used to evaluate the performance of the membranes. This filtration cell has an effective area of 19.6 cm^2. The concentrations of salt solutions were measured by a conductivity meter (Mettler-Toledo). The concentration of raffinose solution was measured by High Performance Liquid Chromatography (HPLC, Shimadzu) using an NH_2 column and a refractive index detector (Shimadzu RI-10A). The concentrations of congo red dye, methyl blue dye and direct red 80 dye were determined with UV-Visible Spectrophotometer (UV-7502C, Shanghai Xinmao Instrument Co, Ltd., China). The rejection rate and permeate flux of the membrane were calculated using the following equations:

$$R = 1 - \frac{C_p}{C_f}$$

$$F = \frac{V}{A\,t}$$

Where C_f and C_p are the concentrations of feed and permeate solutions, V is the volume of the solution permeated in the time period t, A is the effective membrane area, and t is the operational time, respectively. The reported data were the averages of measurements of at least three replicates.

Table 1 Characterization of dyes in the study

Dyes	MW(g mol^{-1})	Charge	Molecular formula	Peak adsorption wavelength(nm)
Congo red	696.66	Negative	$C_{32}H_{22}N_6Na_2O_6S_2$	498
Methyl blue	799.80	Negative	$C_{37}H_{27}N_3Na_2O_9S_3$	627
Direct red 80	1373.07	Negative	$C_{45}H_{26}N_{10}Na_6O_{21}S_6$	528

3 Results and discussion

3.1 Membrane surface characterization

3.1.1 Surface morphology

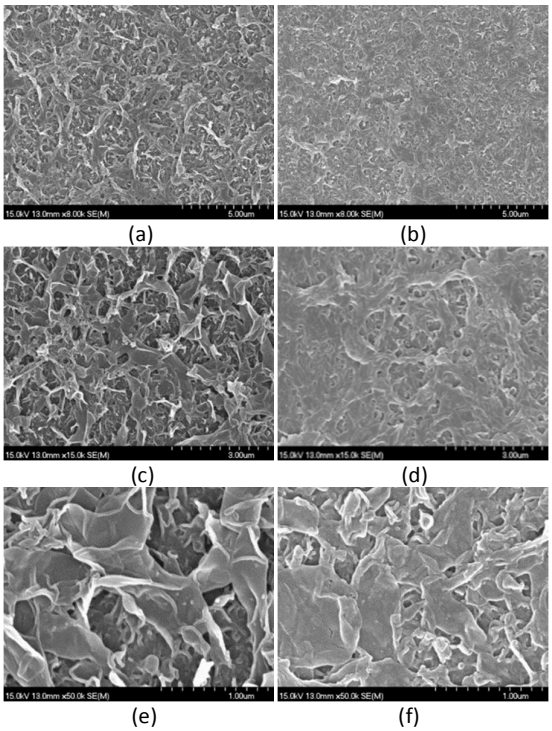

Fig. 1 Surface SEM images of the active layer of (a, c, e) the original RO membrane and (b, d, f) chlorinated RO membrane.

In Fig. 1, SEM pictures of the original and chlorinated RO membranes are shown under different magnifications. The images show that the surfaces of chlorinated membranes (Fig. 1 (b), (d) and (f)) are more planar than original membranes (Fig. 1 (a), (c) and (e)). This indicates that the surface of membranes might be degraded after sodium hypochlorite exposure.

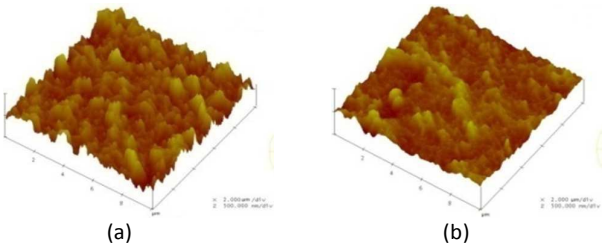

Fig. 2 Surface AFM morphology of the active layer of the original RO membrane (a) and chlorinated RO membrane (b).

The corresponding AFM pictures of the original and chlorinated RO membranes are shown in Fig. 2. The mean roughness and root mean square roughness of the original RO membrane were 68.2 ± 5.8 nm and 86.9 ± 8.1 nm, respectively. After chlorination, the surface roughness of RO membranes has significantly changed, and the mean roughness and root mean square roughness of the chlorinated membrane were 34.7 ± 1.3 nm and 45.0 ± 2.1 nm. Thus, the surface of the membranes after hypochlorite exposure was degraded, which is consistent with the interpretation of the SEM images (Fig. 1). And the degradation occurring in polyamide active layer of the chlorinated RO membrane may cause the change of pore size.

3.1.2 Surface chlorine composition

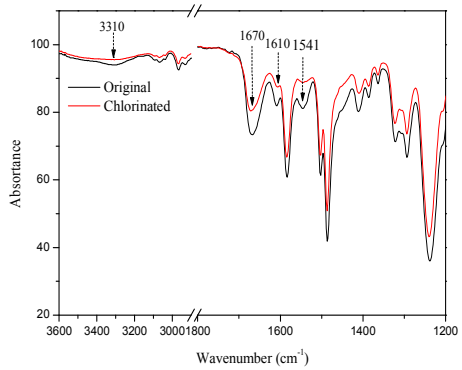

Fig. 3 FT-IR spectra of the original and chlorinated RO membranes.

The variation of the FT-IR spectra of the chlorinated RO membrane is presented in Fig. 3. Four characteristic peaks were observed at 1670 cm^{-1} (amide Ⅰ, C=O stretching), 3310 cm^{-1} (amide Ⅱ, N-H stretching), 1541 cm^{-1} (amide Ⅱ, N-H in-plane bending) and 1610cm^{-1} (C=C ring stretching). As presented in Fig. 3, the intensities of the peaks at 1541 cm^{-1}, 3310 cm^{-1} and 1610 cm^{-1} decrease apparently after sodium hypochlorite exposure. In addition, it can be seen that the amide Ⅰ band at 1670 cm^{-1} shifted slightly to a higher frequency after a few hours of chlorination. These spectral changes indicates that hydrogens in amide nitrogen and aromatic rings are replaced by chlorine, which may cause the destruction of hydrogen bonds between C=O and N-H thereby leading to membrane degradation.[8, 9, 17] This further confirms that RO membranes are partially degraded after hypochlorite exposure.

The XPS full-scan spectrum (Fig. 4(a)) indicates that polyamide active layer of the original RO membrane contains oxygen (at 532 eV), nitrogen (at 398 eV) and carbon (at 285 eV), and their atomic contents are 13.8 %, 12.6 %, and 73.6 %,

respectively. Chlorine was detected at 271 eV (2s) and 200 eV (2p) on the hypochlorite treated membrane surface. The content of chlorine (2p) is 1.8 % on the chlorinated RO membrane, indicating that the active layer surface of the polyamide RO membrane has been chlorinated.[18] In contrast, chlorine was not found on the polyamide active layer of the original RO membrane. As shown in Fig. 4 (b), there are two peaks in the Cl2p spectrum at binding energies of about 197.4 eV and 200.5 eV. The peak of 197.4 eV could be attributed to C_6H_5Cl, the other peak at a binding energy of about 200.5 eV corresponds to O=C-N-Cl. Furthermore, it shows that the chlorinated polyamide RO membrane contains higher quantities of C_6H_5Cl than O=C-N-Cl. Besides that, the O/N ratio indicates the degree of polyamide cross-linking. In theory, the ratio of O/N is 1:1 for a fully cross-linked polyamide layer and 2:1 for a linear polyamide layer. As shown in Table 2, the O/N ratio of RO membrane increases from 1.1 ± 0.1 (original) to 1.9 ± 0.2 (chlorinated), which indicates that the chlorinated membranes are less cross-linked and that more amide bonds are destroyed. The increase of the O/N ratio content is probably due to amide bond hydrolysis, which results in additional carboxylic acid groups. As reported by Kang and Zhai[4, 19], chlorine substitutes for the N-H hydrogen in amide which forming an N-chlorinated intermediate at first, which can not only reversibly regenerate into the initial amide but also rearrange to a ring-chlorinated product via irreversible orton rearrangement gradually, and the ring-chlorinated product may result in amide bonds cleavage thereby causing membrane degradation. And the mechanism of chlorination in polyamides is shown in Fig. 5. The ATR-FTIR and XPS observation also make clear that the surface of the RO membranes was partially degraded after sodium hypochlorite exposure.

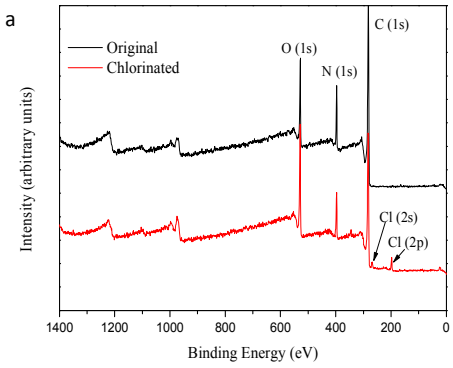

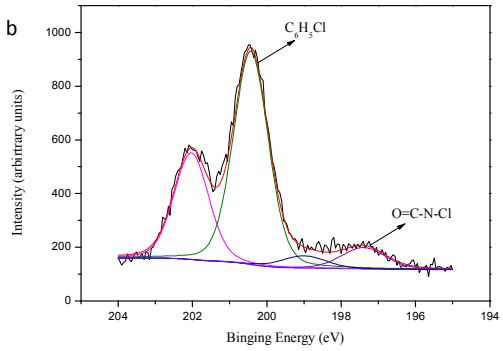

Fig. 4 (a) XPS full-scan spectra of the original and chlorinated RO membrane; (b) Cl2p spectra of chlorinated RO membrane.

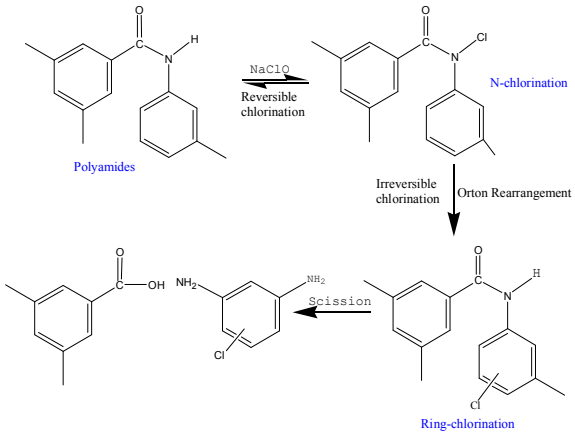

Fig. 5 Proposed mechanism of chlorination in polyamides.

3.1.3 Membrane wettability and streaming potential

Table 3 Contact angle of the original and chlorinated RO membrane

Membrane	Contact angle (°)
Original membrane	50.2 ± 0.8
Chlorinated membrane	45.8 ± 1.0

The hydrophilicity of the membrane surface was analyzed by contact angle measurement. The lower the contact angle, the more hydrophilic of the membrane surface. The contact angle of membranes decreases slightly after sodium hypochlorite exposure (Table 3), indicating that membrane surface becomes more hydrophilic than original membranes. Kwon et al. suggested that this is result from the chlorination of the polyamide active layer of the RO membrane, which leads to a more polar membrane surface. [8, 11] As a result, this may cause an increase of the flux of the chlorinated RO membrane.

Table 2 Elemental composition by atomic percent of original and chlorinated RO membranes

Membrane	O (%)	N (%)	C (%)	Cl (%)	O/N
Original membrane	13.8 ± 0.7	12.6 ± 0.6	73.6 ± 0.2	0	1.1 ± 0.1
Chlorinated membrane	20.0 ± 0.7	10.7 ± 0.5	67.5 ± 0.1	1.8 ± 0.2	1.9 ± 0.2

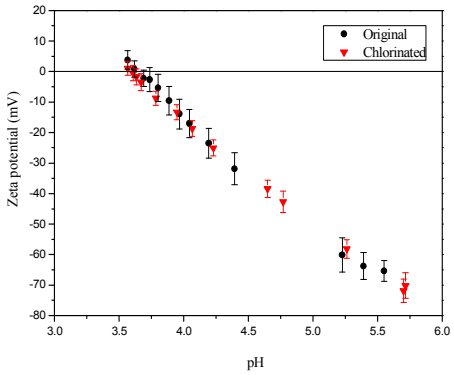

Fig. 6 Zeta potential of the original and chlorinated RO membrane in various pH values.

The charge properties of the RO membrane surface have a significant influence on the membrane performance. As shown in Fig. 6, the isoelectric point of the original and chlorinated RO membrane is 3.7 and 3.6, respectively. Due to chlorine treatment, the hydrogen in amide nitrogen can be replaced by chlorine, thus forming non-hydrogen bonding N-Cl groups.[8] The reduction in the number of amine N-H group can result in a slightly decreased isoelectric point, as suggested in Figure 6. In addition, destruction of the polyamide chain resulted from chlorine treatment may make for the increase of free carboxylic acid groups, thereby leading to a more negative zeta potential.[20]

3.2 Performance characterization

3.2.1 NaCl and Na_2SO_4 rejection

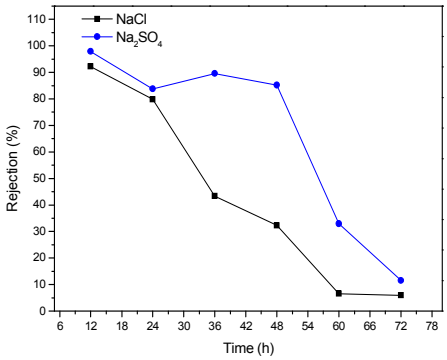

Fig. 7 Effect of soaking time on the performance of abandoned RO membrane.

The effect of the abandoned conditions on nanofiltration performance was investigated by the rejection of inorganic salts NaCl and Na_2SO_4. Membranes used in this experiment were immersed in beakers containing a sodium hypochlorite solution of 1000 ppm for different time at constant temperature (27 °C). And experiments were performed with solution containing 500 mg/L NaCl, 500 mg/L Na_2SO_4 at 0.8 MPa. As shown in Fig. 7, the abandoned RO membranes have the function of nanofiltration for between 36 h and 48 h. In addition, the abandoned RO membranes will gradually lost the function of nanofiltration for more than 48 h, and this result also indicates that the rejection of NaCl and Na_2SO_4 for abandoned RO membrane that exposed to 1000 ppm NaClO solution for 72 h is 5.96 % and 11.55 %, and it shows that the abandoned RO membranes lose the function of nanofiltration on this condition. Therefore, in this study, I recovered the abandoned RO membranes as nanofiltration functional membranes in 48000 ppm h condition.

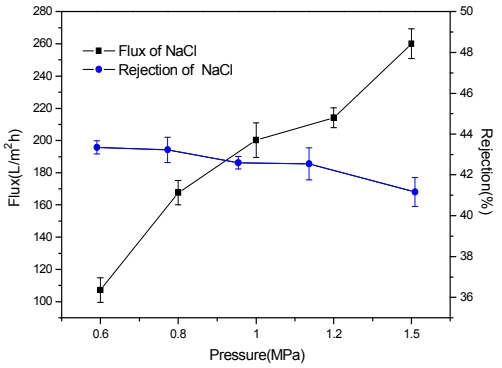

Fig. 8 Performance of a chlorinated membrane for NaCl solution at variable operating pressures.

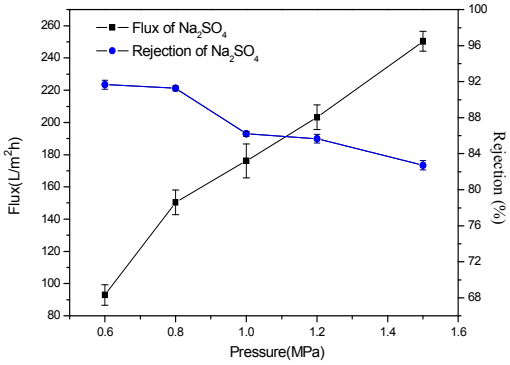

Fig. 9 Performance of a chlorinated membrane for Na_2SO_4 solution at variable operating pressures.

The separation performance was investigated by the permeate flux and rejection of the inorganic salts NaCl and Na_2SO_4. The permeate flux and rejection of NaCl and Na_2SO_4 for chlorinated membranes as a function of operational pressure are presented in Fig. 8 and Fig. 9. The permeate flux of the NaCl and Na_2SO_4 solutions shows an almost linear increase with the operational pressure, while the rejection of NaCl and Na_2SO_4 decreases when the operational pressure increases from 0.6 to 1.5 MPa. On the basis of the Kedem-Katchalsky equation, the permeate flux is proportional to the operational pressure. In addition, a similar phenomenon has been reported by Deng et al, where the rejection of inorganic salts also decreased with

increasing operational pressure. They suggested that the surface forces play a vital role in retaining the ions which is typical in nanofiltration (NF). These forces are constant when the operational pressure increases, but the drag force becomes greater because of higher flux in the pore. Meanwhile, the effect of surface forces becomes almost negligible for the chlorinated membranes, and the solute flux increases, thus the difference between the solute and solvent flux gets diminution, which in turn decrease the rejection rate.[21] In addition, the rejections of NaCl and Na_2SO_4 for the chlorinated membrane are 42.6 % and 86.2 %, respectively. This typical NF behavior demonstrates that abandoned RO membranes after hypochlorite exposure can be recovered as "nanofiltration functional membranes".

3.2.2 Rejection of organic solutes

To investigate the chlorinated membrane performance in purification of solutions containing organic compounds, experiments were conducted with three different dyes and raffinose at 1.0 MPa at room temperature. The separation performance of the "nanofiltration functional membranes" is listed in Table 4. The rejection for direct red 80 (1373.1 g/mol, negative) was 100 %, the rejection for congo red (696.7 g/mol, negative) and methyl blue (799.8 g/mol, negative) was 99.4 % and 98.0 %, respectively. In addition, the rejection for raffinose (504.4 g/mol, neutral) was 72.3 % and thus much lower than that of congo red (696.7 g/mol, negative). This indicates that the main factors affecting the rejection of the chlorinated membrane are not only size exclusion but also charge repulsion which is again typical in NF. However, it can be seen that the rejection for methyl blue (799.8 g/mol, negative) with higher molecular weight is lower than for congo red (696.7 g/mol, negative). Methyl blue is prone to bringing about a foaming effect under operational condition, which causes concentration polarization and membrane fouling on the surface of membranes and induces a lower flux, and results in a lower rejection.

The decolorization effect of "nanofiltration functional membranes" is shown in Fig. 10. It shows that the permeated solution of the membranes is colorless when a direct red 80 solution is filtered, however, the permeated solutions of the membrane are slightly colored when methyl blue and congo red are treated. Thus, nanofiltration functional membranes have an excellent performance for purification of dye solutions. However, the images of the membranes after dye separation indicate the chlorinated membranes also have membrane fouling phenomenon.

Table 4 Performance of a nanofiltration functional membrane for solution containing dyes and raffinose (at 1.0 MPa and room temperature)

Dye and sugar	Charge	MW (g/mol)	J (L/m^2h)	Rejection (%)
Raffinose	Neutral	504.4	189.5	72.3
Congo red	Negative	696.7	168.2	99.4
Methyl blue	Negative	799.8	134.6	98.0
Direct red 80	Negative	1373.1	214.1	100

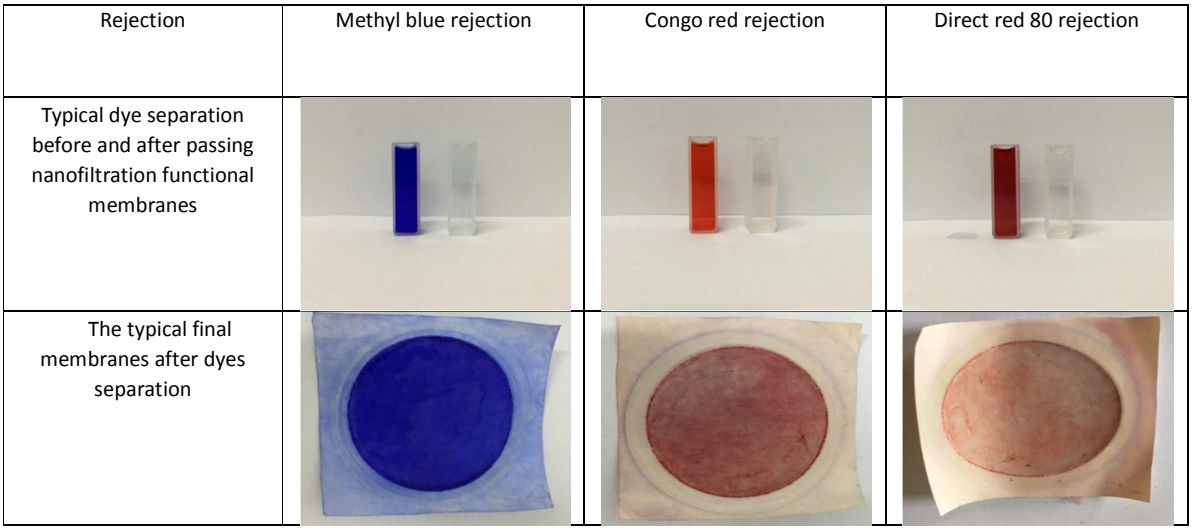

Fig. 10 Images of the feed and permeate after dye separation and membranes after dyes separation.

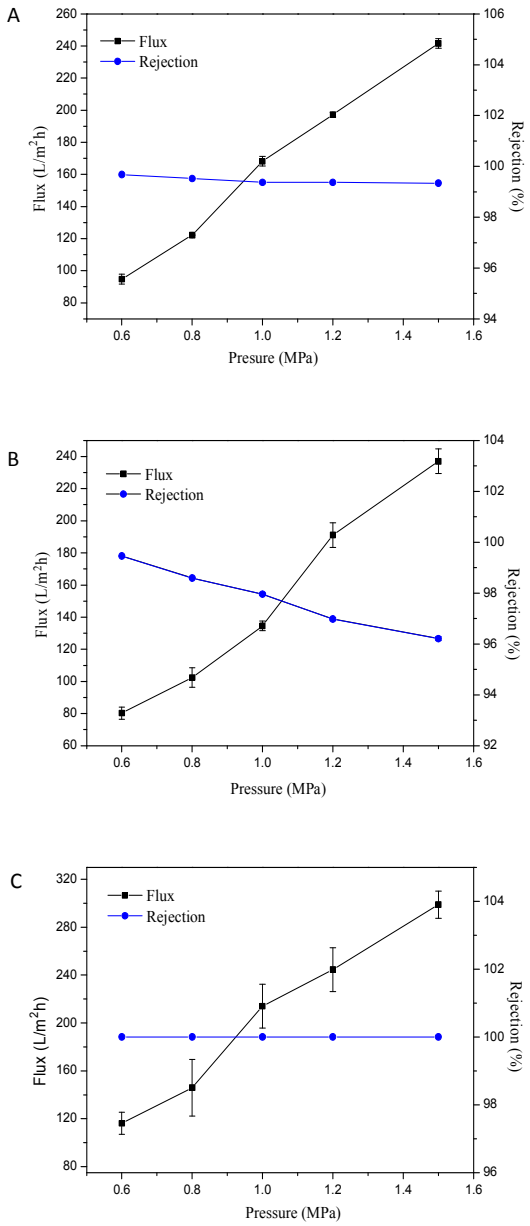

Fig. 11 Effect of operational pressure on dye removal for nanofiltration functional membranes. (A) Congo red; (B) Methyl blue; (C) Direct red 80

To study the chlorinated membrane performance in purification of dye solutions, experiments were conducted with 200 mg/L of three different dyes at different operational pressures. Fig. 11 shows that as the operational pressure increases from 0.6 MPa to 1.5 MPa, the permeate fluxes of congo red, methyl blue and direct red 80 solutions increase significantly, while the rejection for dye has no obvious change. For congo red, as an example, the flux increases from 94.8 L m^{-2} h^{-1} to 241.6 L m^{-2} h^{-1}, while the rejection remains between 99.3 % and 99.7 %. This indicates that the operational pressure plays an important role on the permeate flux. With the increase of operational pressure, the driving force for solutions to across the membrane increased accordingly, therefore, the permeate flux of the membrane increased.[22] Besides that, the stable rejection of dye mainly is due to size exclusion mechanism.

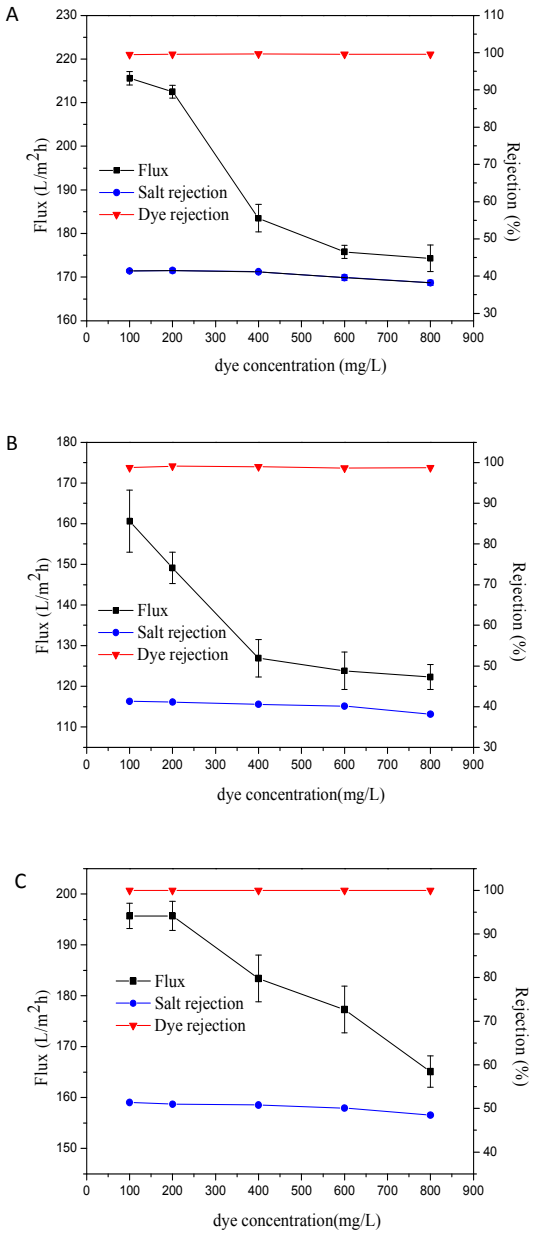

Fig. 12 Effect of feed dye concentrations on permeate flux and the rejection of dye and salt for nanofiltration functional membranes in 1000 mg/L NaCl solution at 1.0 MPa. (A) Congo red; (B) Methyl blue; (C) Direct red 80

Desalination of dye solutions was studied at different dye concentrations in the feed and a fixed NaCl concentration of 1000 mg/L. The variations in permeate flux and the rejection of dye and salt for three different dye solutions are shown in Fig. 12. It can be seen that the feed dye concentration plays a significant role on the permeate flux, while the dye rejection and salt rejection do not change substantially. Taking congo red dye as an example, the permeate flux of the "nanofiltration functional membranes" decreases from 215.6 L m^{-2} h^{-1} to 174.3 L m^{-2} h^{-1} with increasing feed dye concentration. This is because the increase of dye concentration may deposit more dyes on the membrane surface, which leads to concentration polarization and membrane fouling, and eventually decrease the permeate flux.[23] However, the dye rejection of the "nanofiltration functional membranes" remains at about 99.5 % to 99.6 % and the salt rejection also remain unchanged.

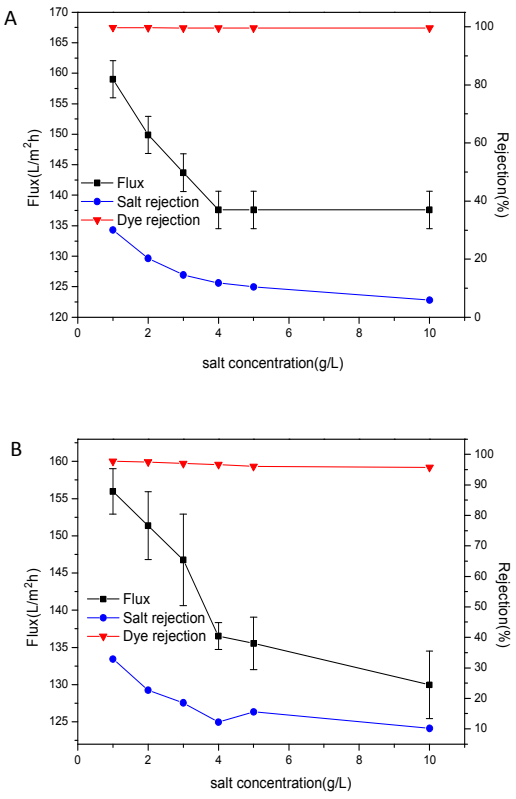

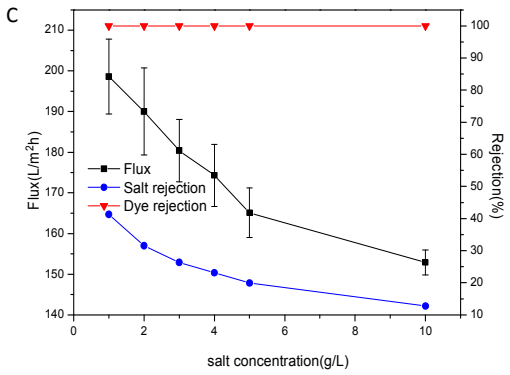

Fig. 13 Effect of feed salt concentrations on permeate flux and the rejection of dye and salt for nanofiltration functional membranes in 200 mg/L dye solution at 1 MPa. (A) Congo red; (B) Methyl blue; (C) Direct red 80

The influence of salt concentration on desalination of dye solution was investigated with different NaCl concentrations in the feed and a fixed dye concentration of 200 mg/L. The research results for three different dye solutions are presented in Fig. 13. For these three dye solutions, the permeate flux and salt rejection of "nanofiltration functional membranes" both decrease with increasing salt concentration, while the salt concentration has an insignificant impact on dye rejection. This is a typical NF behavior. For congo red dye, the salt rejection decreases from 30.0 % to 5.9 % and the permeation flux changes in a narrow range from 159 L m^{-2} h^{-1} to 137.6 L m^{-2} h^{-1}, while the dye rejection remains at about 99.5 % to 99.7 %. The decline of the permeate flux may be caused by two main reasons. On one hand, higher salt concentrations can lead to concentration polarization on the surface of the membrane, which will lead to a decline of the permeate flux. On the other hand, more salt will lead to higher osmotic pressure on both sides of the membrane. At constant operational pressure, the net transmembrane pressure tends to decrease, which also causes the flux decrease. Meanwhile, the decrease of salt rejection can be attributed to the addition of a large quantity of salt, which weakens the electrostatic repulsive interactions between Na^+ and the surface charges of membrane, a phenomenon called the "shield effect". In this case, the size exclusion mechanism plays a dominant role in dye retention over the "shield effect" intensified by NaCl.[14, 24, 25]

3.2.3 Membrane separation performance for desalination of dye solutions

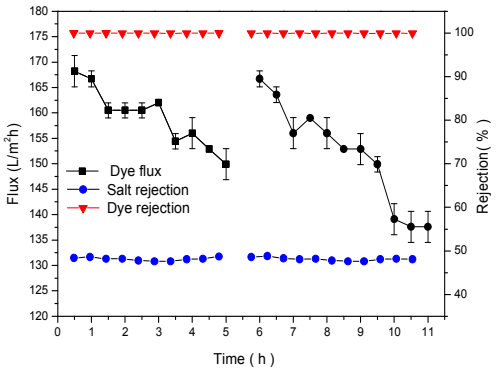

Fig. 14 The performance on desalination and purification of dye solution for a long time.

The performance of "nanofiltration functional membranes" in desalination and purification process for dye solution was further investigated with mixture solution containing 500 mg/L congo red and 1 g/L NaCl at 1.0 MPa. After every 5 h operation, the membrane was rinsed with deionized water for 1 h. Fig. 14 presents the variations in permeate flux and rejection for congo red and the salt rejection of the membrane for 2 consecutive periods of 5 h continuous operation. The result indicates that the permeate flux of the membrane decreases gradually but was rebound at the start of the second period due to the intermediate rinsing. The decrease is due to dye deposition on the membrane surface after a long time of operation. The end flux is 137.6 L m^{-2} h^{-1}, which decreased about 18.2 % compared to the initial flux. This indicates that the "nanofiltration functional membranes" for desalination and purification of dye solutions have good stability.[25, 26]

4. Conclusions

Chlorination promoted degradation of aromatic polyamide reverse osmosis (RO) membranes changes the chemical composition and structure of the active layer. This study suggests that abandoned aromatic polyamide reverse osmosis (RO) membranes can be recovered by sodium hypochlorite degradation as "nanofiltration functional membranes". Analysis of the rejection behavior of inorganic salt and dyes reveals that the typical NF performance is caused by size exclusion and charge repulsion. Furthermore, because "nanofiltration functional membranes'' have a large permeate flux and high rejection for dyes, they have an excellent performance and potential application in desalination and purification of dye solutions.

5. Acknowledgements

The research was supported by the National High Technology Research and Development Program 863 (No. 2015AA030502), the Public Welfare Project of the Science and Technology Committee of Zhejiang Province (No. 2015C31050), Natural Science Foundation of Zhejiang Province (No. Y16B060039). The authors are also grateful to Professor Guoliang Zhang's helpful comments.

References

1. K. P. Lee, T. C. Arnot and D. Mattia, Journal of Membrane Science, 2011, 370, 1-22.
2. J. S. Baker and L. Y. Dudley, Desalination, 1998, 118, 81-89.
3. S. Ebrahim, Desalination, 1994, 96, 225-238.
4. G.-D. Kang, C.-J. Gao, W.-D. Chen, X.-M. Jie, Y.-M. Cao and Q. Yuan, Journal of Membrane Science, 2007, 300, 165-171.
5. M. J. Cran, S. W. Bigger and S. R. Gray, Desalination, 2011, 283, 58-63.
6. S. Ebrahim and H. El-Dessouky, Desalination, 1994, 99, 169-188.
7. V. T. Do, C. Y. Tang, M. Reinhard and J. O. Leckie, Environmental science & technology, 2012, 46, 852-859.
8. Y. N. Kwon and J. O. Leckie, Journal of Membrane Science, 2006, 283, 21-26.
9. Y. N. Kwon and J. O. Leckie, Journal of Membrane Science, 2006, 282, 456-464.
10. A. Ettori, E. Gaudichet-Maurin, J.-C. Schrotter, P. Aimar and C. Causserand, Journal of Membrane Science, 2011, 375, 220-230.
11. V. T. Do, C. Y. Tang, M. Reinhard and J. O. Leckie, Water Research, 2012, 46, 5217-5223.
12. J. Dawei, Z. Jianping, L. Baoguang and j. Wei, Industrial Water Treatment (in Chinese), 2001, 31.
13. E. Forgacs, T. Cserhati and G. Oros, Environment International, 2004, 30, 953-971.
14. R. Jiraratananon, A. Sungpet and P. Luangsowan, Desalination, 2000, 130, 177-183.
15. Y. Ku, P. L. Lee and W. Y. Wang, Journal of Membrane Science, 2005, 250, 159-165.
16. C. Tang and V. Chen, Desalination, 2002, 143, 11-20.
17. Y. N. Kwon, C. Y. Tang and J. O. Leckie, Journal of Applied Polymer Science, 2008, 108, 2061-2066.
18. A. Antony, R. Fudianto, S. Cox and G. Leslie, Journal of Membrane Science, 2010, 347, 159-164.
19. X. Zhai, J. Meng, R. Li, L. Ni and Y. Zhang, Desalination, 2011, 274, 136-143.
20. G. Hurwitz, G. R. Guillen and E. M. V. Hoek, Journal of Membrane Science, 2010, 349, 349-357.
21. H. Deng, Y. Xu, Q. Chen, X. Wei and B. Zhu, Journal of Membrane Science, 2011, 366, 363-372.
22. B. Van der Bruggen, B. Daems, D. Wilms and C. Vandecasteele, Separation and Purification Technology, 2001, 22-3, 519-528.
23. A. Akbari, J. C. Remigy and P. Aptel, Chemical Engineering and Processing, 2002, 41, 601-609.
24. I. Koyuncu, D. Topacik and M. R. Wiesner, Water Research, 2004, 38, 432-440.
25. J. Huang and K. Zhang, Desalination, 2011, 282, 19-26.
26. S. C. Yu, M. H. Liu, M. Ma, M. Qi, Z. H. Lu and C. J. Gao, Journal of Membrane Science, 2010, 350, 83-91.

Graphical Abstract

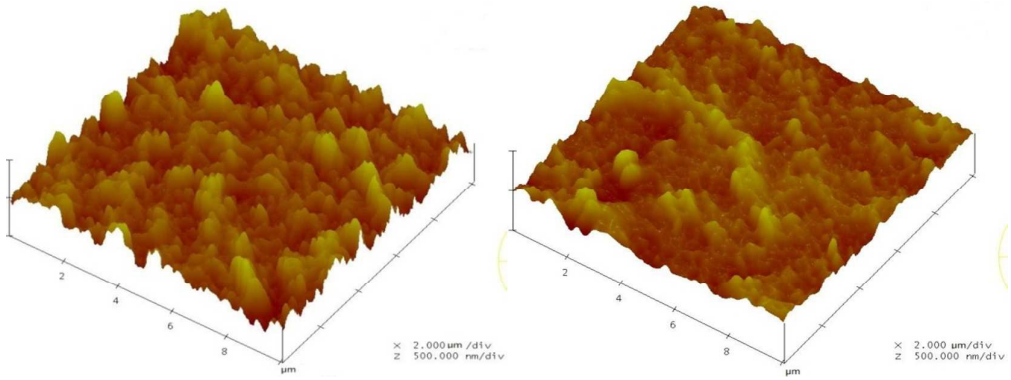

original RO membrane chlorinated RO membrane

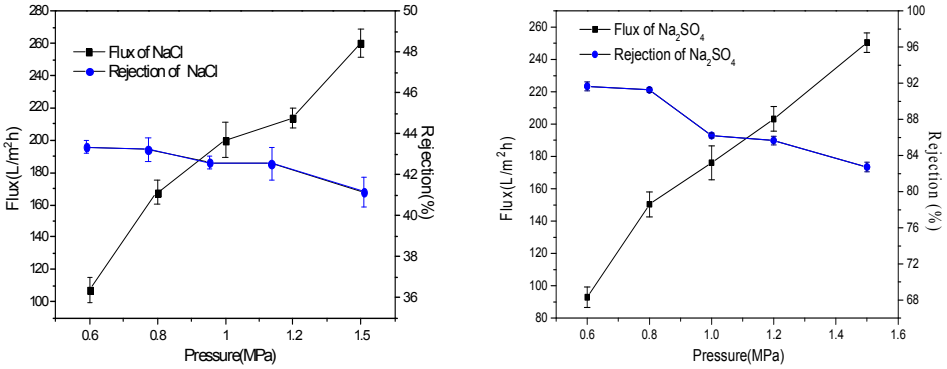

Dye and sugar	Charge	MW (g/mol)	J (L/m^{2}h)	Rejection (%)
Raffinose	Neutral	504.4	189.5	72.3
Congo red	Negative	696.7	168.2	99.4
Methylblue	Negative	799.8	134.6	98.0
Direct Red 80	Negative	1373.1	214.1	100